



Performance and mechanisms of thermally treated bentonite for enhanced phosphate removal from wastewater

Xiang Chen^{1,2,3} · Lu Wu^{1,2,3} · Feng Liu^{1,2} · Pei Luo^{1,2} · Xuliang Zhuang⁴ · Jinshui Wu^{1,2} · Zhenke Zhu^{1,2} · Shengjun Xu⁴ · Guixian Xie⁵

Received: 26 December 2017 / Accepted: 19 March 2018 / Published online: 27 March 2018
© Springer-Verlag GmbH Germany, part of Springer Nature 2018

Abstract

Optimization of clays as adsorbent for low concentration phosphorus removal from wastewater has received increasing attention in recent years. This study explored the feasibility of using bentonite as an adsorbent for phosphate (P) removal from synthetic wastewater, by assessing the performance of thermally treated bentonite for P removal and elucidating the mechanisms of P adsorption. Natural bentonite (B25) was thermally treated at 100–1000 °C (B100–B1000) for 2 h. Physical and chemical properties were measured by the SEM, XRD, pore size distribution, EDX, and cation exchange capacity (CEC) methods. Thermal treatment increased P sorption capacity of bentonite and that B800 had a higher P sorption capacity (6.94 mg/g) than B25 (0.237 mg/g) and B400 (0.483 mg/g) using the Langmuir isotherm equation. Study of sorption kinetics indicated that B800 rapidly removed 94% of P from a 10 mg P/L solution and the pseudo-second-order equation fitted the data well. The Ca²⁺ release capacity of B800 (1.31 mg/g) was significantly higher than that of B25 (0.29 mg/g) and B400 (0.40 mg/g) ($p < 0.05$). The initial pH level had a smaller impact on P removal efficiency for B800 than that of B25 and B400. Ca-P was the main fraction of P adsorbed onto B800, and Ca₁₀-P was the main species (41.4%). The main factors affecting the phosphorous adsorption capacity of B800 were changed crystal structure, strong calcium release capacity, and improved stability in different pH solutions. The results demonstrated that thermally treated bentonite (B800) has the potential to be an efficient adsorbent for removal of low-concentration phosphorus from wastewater.

Keywords Thermal treatment · Bentonite · Adsorption · Phosphate · Wastewater

Introduction

Phosphorus is a major nutrient and contaminant in surface water. It mainly comes from agricultural and urban storm runoff, municipal and industrial effluents, and livestock and poultry excreta (Chen et al. 2016a; Luo et al. 2017; Liu et al. 2017). Phosphorus, rather than nitrogen, is reported to be the limiting nutrient for eutrophication in many freshwater ecosystems (Sengupta and Pandit 2011; Chen et al. 2016b). Excessive phosphorus can cause eutrophication in rivers, lakes, and reservoirs (Yeoman et al. 1988; Elser et al. 2007). Many techniques have been applied to remove phosphorus from wastewaters, such as chemical precipitation, biological methods, and adsorption (Vohla et al. 2011; Loganathan et al. 2014). In these methods, adsorption is considered to be a low-cost, environmental friendly, and effective approach for removing low concentrations of phosphate (P) (Gupta et al. 2009). Using clay minerals for phosphate adsorption has been extensively investigated in recent years. Clay minerals are common in

Responsible editor: Guilherme L. Dotto

✉ Feng Liu
liufeng@isa.ac.cn

- ¹ Key Laboratory of Agro-ecological Processes in Subtropical Regions, Institute of Subtropical Agriculture, Chinese Academy of Sciences, Changsha 410125, Hunan Province, China
- ² Changsha Research Station for Agricultural & Environmental Monitoring, Institute of Subtropical Agriculture, Chinese Academy of Sciences, Changsha 410125, Hunan Province, China
- ³ University of Chinese Academy of Sciences, Beijing 100049, China
- ⁴ Key Laboratory of Environmental Biotechnology, Research Center for Eco-Environmental Sciences, Chinese Academy of Sciences, Beijing 100085, China
- ⁵ College of Resource and Environment, Hunan Agricultural University, Changsha 410128, Hunan Province, China

nature and have high specific surface area and high adsorption capacity (Barca et al. 2012, 2013; Yin et al. 2017).

Of the clay minerals, bentonite is an abundant resource worldwide and accounts for nearly 68% of the clay used for sorbents in the control of pollution (Vimonses et al. 2009; Zhu et al. 2016). Bentonite is a typical 2:1-type phyllosilicate clay mineral, which contains one octahedral (O) sheet sandwiched between two tetrahedral (T) sheets (Brigatti et al. 2013). Because of the isomorphous substitution of metal cations in the sheets, the layers carry a permanent negative charge in the surface, which is balanced by cationic counterions in the inter-layer space (see Zhu et al. 2016). The characteristics make bentonite useful as an adsorbent for a wide variety of contaminants, such as cationic pollutants (Aytas et al. 2009; Gupta and Bhattacharyya 2014) and anionic pollutants (Zhu et al. 2009).

Physical and chemical modification of natural bentonite can enhance its adsorption capacity (Ye et al. 2006; Toor and Jin 2012). Thermal treatment has been recognized as a cost-effective modification method for improving the clay minerals adsorption capacity (Gan et al. 2009; Yin et al. 2017). Waters located in intracrystalline tunnels of bentonite can be selectively removed with different calcination temperatures. The changes of the structure and components through multiple stages from dehydration to sintering condition are very important factors affecting the adsorption capacity (Sarıkaya et al. 2000; Stagnaro et al. 2012). Aytas et al. (2009) reported that the bentonite thermal treated at 400 °C had the best adsorption capacity for heavy metal because of the changed specific surface area. However, little information has been reported concerning the effect of thermal treatment on sorption capacity of bentonite to remove phosphorus.

In order to broaden the usage of bentonite and take advantage of its abundance for removal the low-concentration phosphorus, this study explored the feasibility of using bentonite as an adsorbent for phosphate removal from synthetic wastewater. The main aims of this study were (1) to assess the performance of thermally treated bentonite for its P removal ability using batch contact experiments and (2) to elucidate the mechanisms of P adsorption by the natural and thermally treated bentonites.

Materials and methods

Preparation of adsorbents

The material for this study was natural Ca-rich bentonite clay (B25) containing high montmorillonite (80–85%), mined in Zhengzhou, Henan Province, China. The physical properties and chemical composition of B25 are shown in Table 2. The bentonite was ground and sieved to less than 1 mm. Bentonite samples were calcined in a muffle furnace for 2 h, with the temperatures ranging from 100 to 1000 °C, and subsequently

labeled as B100, B200, B300, etc. The thermally treated samples were cooled to room temperature and stored in a desiccator for further use.

Characterization of adsorbents

X-ray diffraction (XRD) patterns of the natural and thermally treated bentonites were recorded by a D/MAX2200 X-ray diffractometer (Rigaku, Japan) with the accelerating voltage of 40 kV, 30 mA, and Cu K α ($\lambda = 0.154178$ nm) radiation ranging from 5 to 80°. The surface structure and chemical composition of the samples were characterized using a field emission scanning electron microscopy (SEM, Hitachi SU8010, Japan) and an energy-dispersive X-ray (EDX, Hitachi SU8010, Japan) spectroscopy. The specific surface area and pore volume of the bentonites were measured using the N₂ adsorption-desorption technique with a Quadrasorb SI (Quantachrome Corporation, USA) and calculated by the Brunauer–Emmett–Teller (BET) and density functional theory (DFT) method, respectively. Micropore volume was calculated by t-plot method using the adsorption data from the interval $0.2 < x (p/p_0) < 0.5$. BET, DFT, and t-plot methods were carried out in the Quantachrome ASIQWin3.0 software. Ammonium acetate method was used to measure the cation exchange capacity (CEC) of the bentonites (Tan 1996).

Phosphate batch adsorption experiments

Evaluation of the P sorption capacity of bentonite

One gram of adsorbent was added to each of three polyethylene centrifuge tubes (100 mL) with a 50 mL KH₂PO₄ solution of 10, 50, and 100 mg/L. After equilibrating for 24 h in the thermostatic shaker (25 °C, 180 rpm), the solutions were centrifuged with an Anke centrifuge (TDL-40 B, Shanghai, China), filtered, and then analyzed for phosphate using the molybdenum blue ascorbic acid method with a UV-Vis spectrophotometer at 882 nm (UV-2300, Shanghai, China) (Soil Science Society of China 2002). The P adsorption capacity of the adsorbent (mg/g) was calculated by Eq. (1):

$$q_e = (C_0 - C_e) V / m \quad (1)$$

where q_e (mg/g) is the equilibrium concentration of phosphate on the adsorbent; C_0 and C_e (mg/L) are the initial and equilibrium concentrations of phosphate in the solution, respectively; m (g) is the mass of adsorbent; and V (L) is the volume of phosphate solution.

Adsorption isotherms of phosphate

One gram of adsorbent was added to 100-mL polyethylene centrifuge tubes, with 50 mL KH₂PO₄ solutions of 1, 5, 10,

20, 40, 60, 80, 100, 150, 200, and 300 mg/L. The solutions were shaken and centrifuged, and the supernatants were filtered and measured. To describe the sorption processes in the P sorption of bentonites, the P sorption isotherms data were fitted by Langmuir isotherm equation (Eq. (2)) and Freundlich isotherm equation (Eq. (3)):

$$1/q_e = 1/q_m + (1/K_L q_m)(1/C_e) \quad (2)$$

$$\ln q_e = \ln K_F + (1/n) \ln C_e \quad (3)$$

where q_m (mg/g) is the maximum sorption capacity of the adsorbent; K_L (L/mg) is the Langmuir constant related to the affinity between an adsorbent and an adsorbate; K_F (mg/g)/(mg/L)ⁿ is the Freundlich constant; and n (dimensionless) is the Freundlich intensity parameter.

Phosphate adsorption kinetics

One gram of the adsorbent was added to 100-mL polyethylene centrifuge tubes with 50 mL of 10 mg/L P solution. Samples of the solutions were retrieved at intervals of 0, 1, 2, 5, 10, 20, and 30 min, and 1, 2, 3, 4, 8, 12, 24, and 36 h. The solutions were centrifuged, filtered, and measured.

Four kinetic equations (Eqs. (4)–(7)) were used to fit the P sorption data and to understand the mechanisms of the adsorption kinetics and the phosphate sorption processes on thermally modified bentonite, as follows:

$$\text{Pseudo-first-order equation (PFO)} : \ln(q_e - q_t) = \ln q_e - k_1 t \quad (4)$$

$$\text{Pseudo-second-order equation (PSO)} : t/q_t = 1/k_2 q_e^2 + t/q_e \quad (5)$$

$$\text{Simple Elovich equation (SE)} : q_t = a + b \ln t \quad (6)$$

$$\text{Intra-particle diffusion (IPD) equation} : q_t = k_p t^{1/2} + c \quad (7)$$

where q_t (mg/g) is the sorption capacity of the adsorbent at any time t ; t (h) is the sorption time; k_1 (1/h) is the rate constant of the PFO equation; k_2 (g/mg × h) is the rate constant of the PSO equation; a (mg/g) and b (mg/g × h) are the desorption constants of the SE equation, respectively; k_p (mg/g × h^{1/2}) and c (mg/g) are the rate constant of the IPD model, respectively.

Ca²⁺ release kinetics

One gram of the adsorbent was added to 100-mL polyethylene centrifuge tubes containing 50 mL deionized water. The solutions were shaken and retrieved for Ca²⁺ release analysis after the following time intervals: 1, 2, 5, 10, 20, and 30 min, and 1, 2, 3, 4, 8, 12, 24, and 36 h. The solutions were centrifuged, filtered, and measured with a 720 ICP-OES (Agilent, CA, USA).

The Ca²⁺ release capacity from bentonite was calculated using the following equation (Eq. (8)):

$$Q_t = C_{Ca}^t V/m \quad (8)$$

where Q_t (mg/g) is the release capacity of Ca²⁺ at any time t ; and C_{Ca}^t (mg/L) is the total Ca²⁺ concentration of the solution at any time t .

Effect of pH on P adsorption

The effect of pH on P sorption by natural and thermally treated bentonite was examined using an initial P concentration of 10 mg/L solution, and samples of the initial P solution were dosed with 0.5 M NaOH and 0.5 M HCl to adjust the pH values to 3, 5, 7, 9, and 11.

Phosphate fractionation of the adsorbed phosphorus

Ten grams of B800 was added into an Erlenmeyer flask with 10 mg/L phosphate solution. The solution was thoroughly mixed and the P saturated B800 was freeze dried and sieved through a 100-mesh sieve for fractionate P analysis. Operationally defined, fractionated P includes six main groups (Gan et al. 2009; Yin et al. 2011): Ca₂-P, Ca₈-P, Ca₁₀-P, Al-P, Fe-P, and O-P.

Statistical analysis

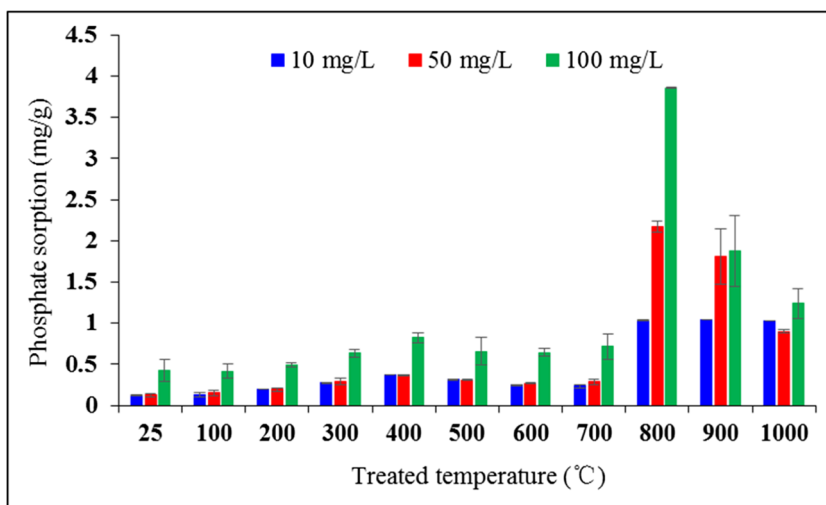
Basic calculations were performed by Microsoft Office Excel. The graphs were plotted by Microsoft Office Excel and Sigmaplot 13. IBM SPSS 23 was used for detailed statistical analysis and the analyses were performed by Mann–Whitney test and one-way ANOVA with Tukey test.

Results

Phosphate sorption capacity of thermally treated bentonites

The effect of calcination temperature on the adsorption capacity of bentonite is presented in Fig. 1. As calcination temperature increased from 25 to 400 °C, the P sorption capacity of bentonite increased slightly ($p > 0.05$) but then decreased slightly ($p > 0.05$) when the calcination temperature increased from 400 to 700 °C. From 700 to 800 °C, the P sorption capacity of bentonite increased significantly ($p < 0.05$) and reached its maximum value. When the temperature increased above 800 °C, the P sorption capacity decreased, becoming especially fast with high P concentration. Based on the P sorption capacity, B25, B400, and B800 were chosen as materials for further research.

Fig. 1 Effects of treated temperature on the phosphate sorption capacity of the bentonite at different phosphate concentrations



Physical and chemical characteristics of bentonite

SEM images of natural (B25) and thermally treated (B400, B800, and B1000) bentonites are shown in Fig. 2. The surface of the B25 (Fig. 2a) appears smooth because of closely packed flakes, in contrast to the irregular platelets in the B800 and B1000. Thermal treatment at 400 °C did not caused any apparent change to the surface structure of bentonite compared to B25. However, with the temperature increased to 800 °C, an increase in particle roughness could be observed. At higher temperatures (> 800 °C), however, the platelet edge has been melted down (Fig. 2d).

XRD results showed that the major minerals identified in the samples were quartz, gismondine, montmorillonite, and sanidine (Fig. 2e). The peak of montmorillonite changed slightly after heating from 25 to 400 °C, and disappeared at 1000 °C. Most crystalline phases in the bentonite also disappeared after heated at 1000 °C (i.e., in B1000), with the exception of quartz. The XRD patterns showed that the degree of d_{001} increased from 5.95 of B25 to 8.86 of B400 and the intensity is reduced after calcination.

As the temperature increased, the BET surface area and micropore surface area values fluctuated (Table 1), increased from 12.87 to 56.09 m²/g, from 0.083 to 7.488 m²/g, respectively, then the values decreased to 30.53 and 4.40 m²/g at 800 °C, respectively. The pore volume and micropore volume value also increased as the temperature increased from 25 to 400 °C, then the value decreased as the temperature increased to 800 °C.

The EDX assay showed that the most abundant elements present in the bentonite samples were Si, O, Al, and Fe, whereas K, Mg, and Ca were found in relatively low amounts (Table 2). As the calcination temperature increased, the percentages of Al, Mg, and Ca also increased, but the percentages of Si and K decreased slightly. Table 1 also shows the change in the CEC of bentonite with increasing calcination

temperature. It is notable that the CEC of B800 was 5.27 cmol/kg, significantly lower ($p < 0.05$) than that of B25 (33.07 cmol/kg) and B400 (28.75 cmol/kg).

Phosphate sorption isotherms and kinetics

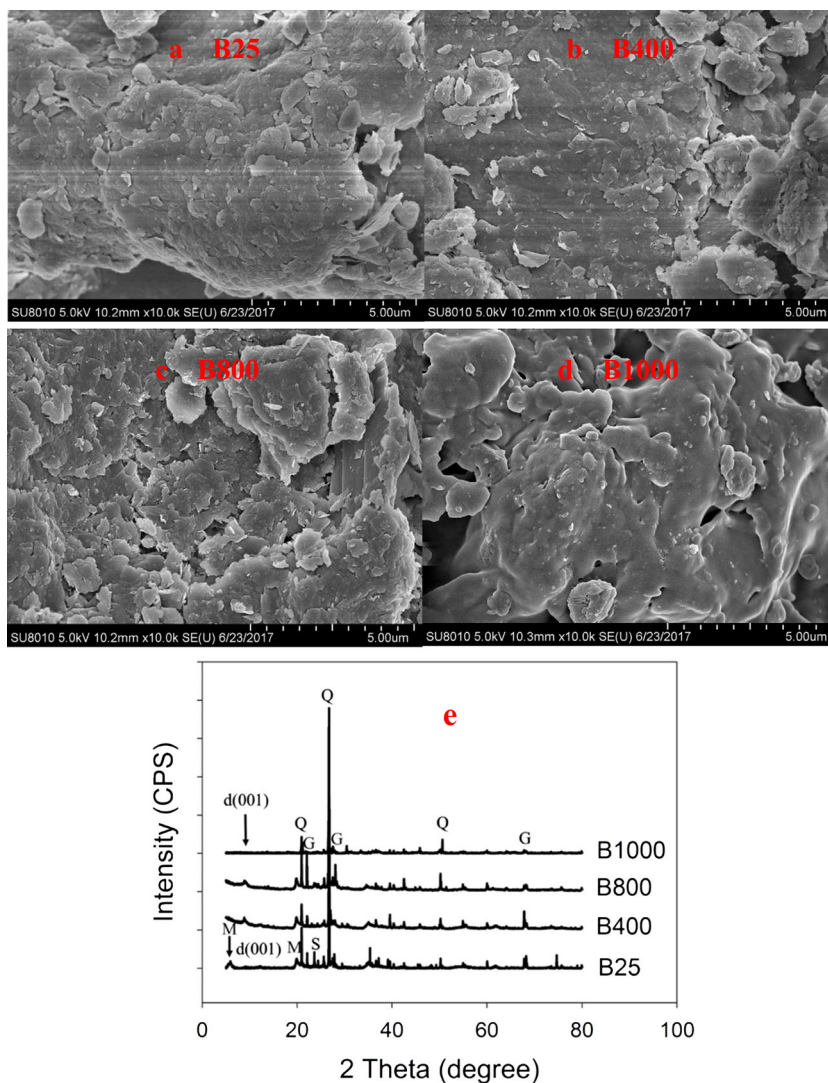
Phosphate sorption isotherms

The P sorption isotherms for natural (B25) and thermally treated (B400 and B800) bentonites are presented in Fig. 3 and Table 3. The results indicated that the P sorption capacity of bentonites increased with the increasing initial P concentration. The P sorption capacity of B800 was higher than that of B25 and B400 at various initial P concentrations. The P removal efficiency of the thermally treated bentonites varied at different initial P concentrations. The P removal efficiency of B800 was 94.3–99.8% at the initial P concentrations of 1–40 mg/L, and then decreased sharply from 77.5 to 14.4% when the initial P concentrations increased from 60 to 300 mg/L. Similarly, B25 and B400 had higher P removal efficiencies at 1 mg/L than at other initial P concentrations. The P removal efficiency of B25 and B400 decreased from 28.6 to 2.74% and from 54.7 to 5.54% when the initial P concentrations increased from 60 to 300 mg/L. High R^2 values showed that P sorption data for B25, B400, and B800 can be described by both the Langmuir and Freundlich equations ($R^2 > 0.98$, Table 3), and the Langmuir isotherm model fitted the sorption data better than the Freundlich isotherm model.

Phosphate adsorption kinetics

The amounts of P adsorbed on B25, B400, and B800 over time are shown in Fig. 4a–c, respectively. The results showed a clear difference in P removal process between these bentonites. The P sorption kinetic process of B25 consisted of three steps (Fig. 4a). In step 1, lasting about 10 min after the

Fig. 2 Scanning electron microscope images (a, b, c, and d) and X-ray diffraction patterns (e) of natural (B25) and thermally treated (B400, B800, B1000) bentonites (Q, quartz; M, montmorillonite; G, gismondine; S, sanidine)



addition of the initial P solution to the B25 samples, the P sorption capacity quickly increased. Step 2 lasted for the next 170 min, and the P sorption capacity decreased in this time. In step 3, the P sorption capacity increased very slowly in the rest time (Fig. 4a). B400 had rapid kinetics in the first 5 min (Fig. 4a, step a), but the P sorption capacity decreased sharply from 0.14 to 0.012 mg/g in the following 5 min. From then on, the P sorption capacity increased, until the process was completed and equilibrium reached at about 24 h (Fig. 4b, step b). The P sorption capacity of B800 increased quickly from 0.176 mg/g at 0 min to 0.496 mg/g around 5 min (Fig. 4c, step i), and the

majority of P sorption was complete in about 10 min when it reached equilibrium (Fig. 4c, step II). Four kinetic equations and their estimated parameters with R^2 are shown in Table 4. The P sorption kinetics of B25, B400, and B800 could be satisfactorily described by the PSO equation ($R^2 > 0.982$).

Ca²⁺ release kinetics

The kinetics of Ca²⁺ release for B25, B400, and B800 are shown in Fig. 5. The results illustrated that B800 can release higher concentrations of Ca²⁺ than B25 and B400. After 8 h,

Table 1 The variation of the BET and pore volume of thermal-treated bentonite as calculated from the adsorption and desorption data of N₂ at liquid N₂ temperature

Number	BET surface area (m ² /g)	Micropore surface area (m ² /g)	Pore volume (cm ³ /g)	Micropore volume (cm ³ /g)
B25	12.87	0.083	0.023	0.00028
B400	56.09	7.488	0.061	0.007
B800	30.53	4.40	0.051	0.0021

Table 2 Physical properties and chemical composition of natural (B25) and thermally treated (B400, B800) bentonites

Properties	Mass of bentonite (%)		
	B25	400 °C	800 °C
Si	30.509	27.550	26.815
O	26.389	29.395	26.488
Al	14.863	15.179	16.101
Fe	10.998	8.720	10.872
K	2.684	2.424	1.656
Mg	2.590	2.813	4.690
Ca	1.366	2.149	2.415
CEC (cmol/kg)	33.07	28.57	5.27

the Ca²⁺ release of B800 reached equilibrium at a concentration of approximately 26 mg/L, significantly higher than the equilibrium Ca²⁺ concentrations of B25 (5.83 mg/L, *p* < 0.05) and B400 (7.99 mg/L, *p* < 0.05), and it slightly decreased after 24 h. The Ca²⁺ release capacity of B800 was 1.31 mg/g, significantly higher than that of B25 (0.29 mg/g, *p* < 0.05) and B400 (0.40 mg/g, *p* < 0.05).

Effect of pH on P sorption

The pH could significantly influence the P sorption capacity of the adsorbents (Fig. 6). The P sorption capacity of B25 was lowest when used with an initial solution with pH 7. For B400, as the pH value increased, the P sorption capacity decreased significantly from its maximum sorption capacity of 0.178 mg/g at pH 3 to 0.076 mg/g at pH 11 (*p* < 0.05). For B800, the P sorption capacity decreased slightly as pH value increased.

Figure 6 also shows a comparison of changes between the initial and the equilibrium pH values. The results suggested that when the initial pH value was lower than 7, the equilibrium pH value was much higher than the initial pH value after the P adsorption process. When the initial pH value was

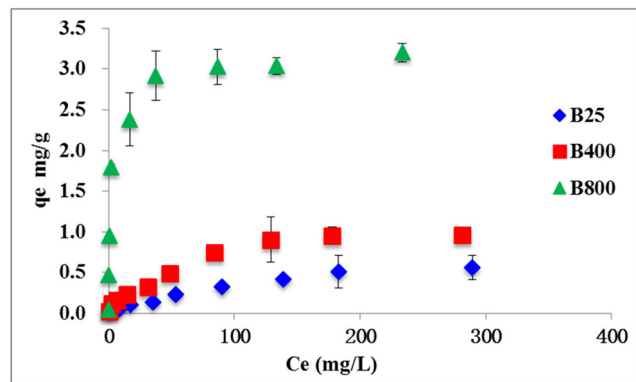


Fig. 3 Sorption data of natural (B25) and thermally treated (B400, B800) bentonites

Table 3 Isotherm parameters of equilibrium phosphate sorption onto natural (B25) and thermally treated (B400, B800) bentonites

	Langmuir model			Freundlich model		
	<i>q_m</i> (mg/g)	<i>K_L</i> (L/mg)	<i>R</i> ²	<i>K_F</i> (mg/g)/(mg/L) ^{<i>n</i>}	<i>n</i>	<i>R</i> ²
B25	0.237	0.085	0.986	0.015	1.475	0.983
B400	0.483	0.132	0.992	0.051	1.724	0.984
B800	6.944	0.128	0.998	1.511	5.848	0.980

increased from 3 to 11, the equilibrium pH value of B25 and B400 increased from 7 to 10. However, when the initial pH value was increased from 3 to 9, the equilibrium pH value of

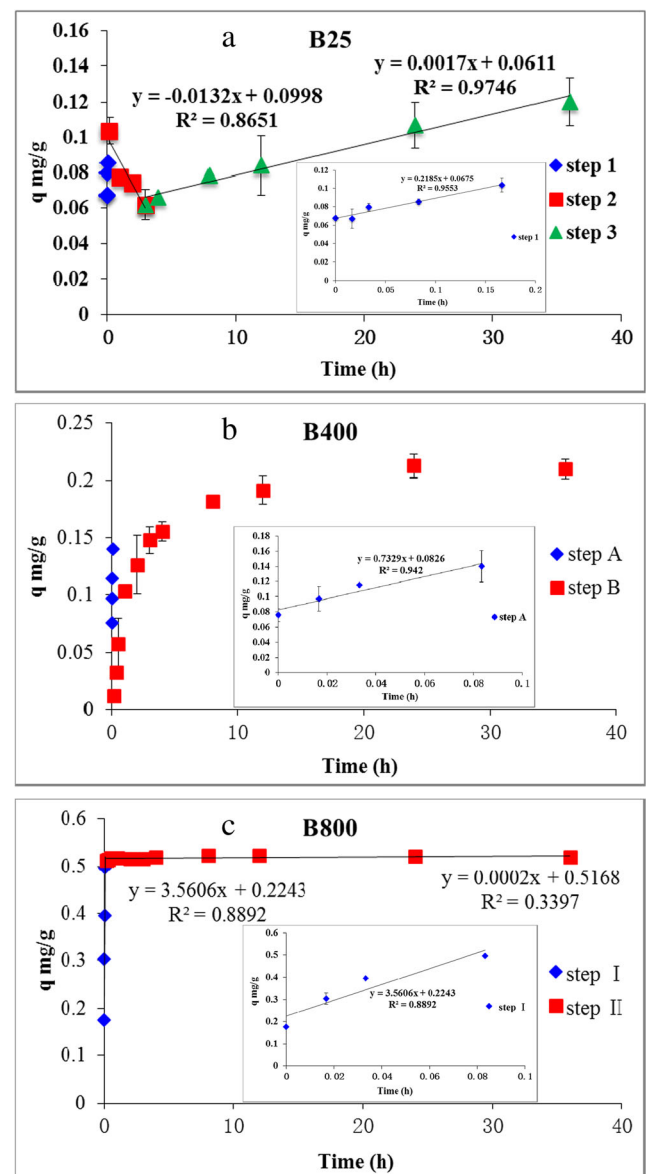


Fig. 4 Kinetics data of natural (a B25) and thermally treated (b B400, c B800) bentonites

Table 4 The kinetic parameters of equilibrium phosphorus sorption onto natural (B25) and thermally treated (B400, B800) bentonites

	Pseudo-first-order equation			Pseudo-second-order equation			Elovich equation			Intraparticle diffusion equation		
	q_1 (mg/g)	k_1 (1/h)	R^2	q_2 (mg/g)	k_2 (g/(mg h))	R^2	a (mg/g)	b (mg/(g h))	R^2	K_p (mg/(g h ^{0.5}))	C (mg/g)	R^2
B25	0.10	0.25	0.689	0.11	7.92	0.982	0.002	0.082	0.106	0.005	0.072	0.359
B400	0.25	0.53	0.441	0.21	6.67	0.997	0.041	0.091	0.979	0.026	0.079	0.629
B800	0.78	48.3	0.955	0.52	229	1.000	0.093	0.701	0.945	0.867	0.201	0.926

B800 remains at 10.6 and increased slightly when the initial pH value increased to 11.

Phosphate fractionation of the adsorbed phosphorus

The P fractionation was distributed as follows: Ca₁₀-P, 41.4%; Al-P, 21.8%; Ca₈-P, 20.6%; Ca₂-P, 13.6%; Fe-P, 2.61%; and O-P, 0.08% (Fig. 7). It showed that Ca-bound P forms and Al-P accounted for most of the total phosphorus, and the species of Ca₁₀-P was the main form of occurrence in the P fractionation. The capacity for sorption of Ca₁₀-P was 0.19 mg/g, significantly higher than that of the other Ca-bound P forms Ca₂-P and Ca₈-P ($p < 0.05$).

Discussion

The difference P sorption capacity of the bentonites can be explained by the change of structural and textural properties (Fig. 2, Table 1, and Table 2). As the temperature increased to 400 °C, no apparent changes occurred in the surface morphology of the bentonite (Fig. 2b) but the crystal structure changed and the space distance declined from 1.49 to 1.00 nm after calcination (Fig. 2e). However, the P sorption capacity of bentonite increased when the temperature increased from 25 to 400 °C because of reversible dehydration (Sarıkaya et al. 2000; Önal and Sarıkaya 2007; Tămășan et al. 2010). While, as the temperature increased up to 800 °C, the space of the layers was not changed but the bentonites loss their hydroxyls

(Chorom and Rengasamy 1996; Emmerich 2000). The dehydration and dehydroxylation could be measured by thermogravimetric analysis and differential thermal analysis (DTA-TG) method, which may contribute to opening the inside channels of bentonite and providing more adsorption sites (Al-Asheh et al. 2003) and it supported by the increasing BET surface area and pore volume value (Table 1). However, the P sorption capacity was declined when the temperature increased to 1000 °C, and the BET and CEC value decreased (Table 1, Table 2). The higher temperature caused complete collapse of micro pores and the shifting of the average pore diameter towards larger values (Zuo et al. 2017; Ortega 2009). In addition to these structural changes, calcination also changed the textural properties of bentonite and influenced its dispersibility in water, which were important for removal of a wide variety of contaminants (Toor and Jin 2012).

The isotherm data indicated that the P adsorption of B25, B400, and B800 could be fitted by both the Langmuir and Freundlich models; the Langmuir isotherm model yields a better fit to the experimental data. This indicated that the surface of bentonite provides both homogeneous monolayer and heterogeneous active sites for P adsorption (Yin et al. 2016); moreover, the homogeneous monolayer adsorption was the dominant mechanism for P adsorption on bentonites. The Langmuir isotherm model showed that the R^2 value increased with increasing treatment temperature (Table 3). The results showed that B800 had a higher P sorption capacity (6.94 mg P/g) than natural bentonite clay (0.24 mg P/g), or the thermal-

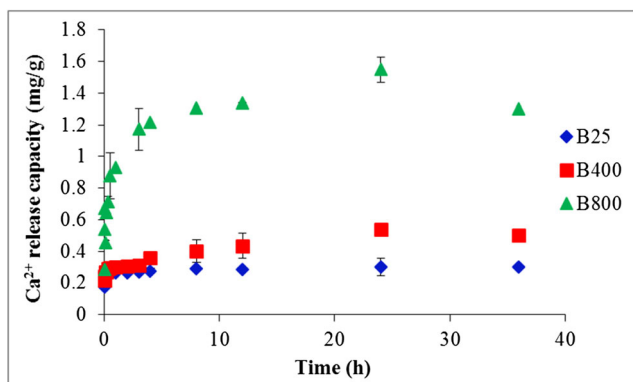


Fig. 5 Kinetics of Ca²⁺ release from natural (B25) and thermally treated (B400, B800) bentonites

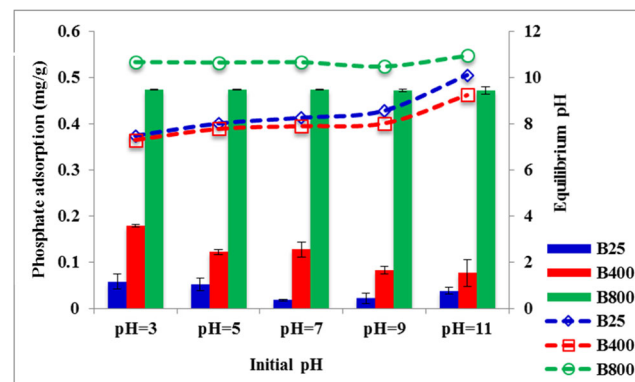


Fig. 6 Effect of pH value on phosphate sorption capacity of natural (B25) and thermally treated (B400, B800) bentonites

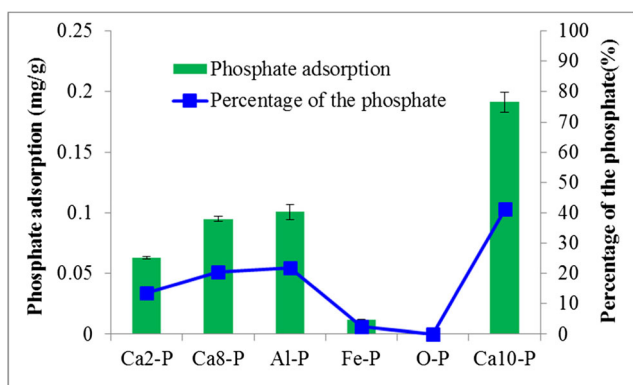


Fig. 7 Phosphate fractionation in discrete chemical forms

modified Ca-rich attapulgite (5.99 mg P/g) used by Yin et al. (2016). High P sorption capacity indicated that Ca-rich bentonite thermally treated at a temperature of 800 °C may be a promising adsorbent in wastewater treatment.

For natural clay minerals, there are four stages associated with transport processes during adsorption: bulk transport, film diffusion, intraparticle diffusion, and adsorptive attachment, which are affected by the pore structure and the pore wall surface (Walter 1984; Weber and Smith 1987; Tran et al. 2017). In this research, three steps were observed for phosphate adsorption with B25. With B400, three steps also existed, but the second “film diffusion” stage was shorter, because the thermal treatment had affected the external surface and pore structure of the bentonite. With B800, however, the pore volume was further enlarged, and the adsorption equilibrium of B800 was quickly established in about 10 min, faster than that of B25 and B400. The equilibrium time has an important effect on the P removal efficiency and costs for adsorbents (Chouyyok et al. 2010; Yin et al. 2011). The equilibrium time of B800 used in the present study was shorter than that of other Ca-rich clay adsorbents, which required several hours or days (Kaasik et al. 2008; Rentz et al. 2009; Yin et al. 2011). The variation in equilibrium times among the bentonites may be attributed to their structure change by thermal treatment, which results in different sorption processes and mechanisms. The P sorption kinetics of B25, B400, and B800 can be satisfactorily described by the pseudo-second-order model (Table 4), indicating that chemical precipitation is the main mechanism of phosphate sorption on the bentonites. This finding is similar to that of other studies that reported the adsorption mechanisms of P on modified clay minerals (Yin et al. 2016; Yin et al. 2017).

Among the three materials used, B800 had the highest capacity for P removal. One other possible explanation was that B800 could generate more OH⁻ and Ca²⁺ during the P removal process than B25 or B400 (Fig. 5 and Fig. 6). The higher equilibrium pH and Ca²⁺ concentration released by B800 would be more favorable for P removal. This phenomenon is also observed in the use of Ca-rich materials to remove

phosphorus and other pollutants (Chen et al. 2011a, b; Barca et al. 2012, 2013; Blanco et al. 2016).

The pH value could significantly affect the P sorption capacity of the adsorbents during the sorption process (Wei et al. 2008). The increase of pH value from 3 to 11 (acidic to alkaline) influenced the P sorption capacity of B25, B400, and B800 to different extents. It mainly related to the dissolution of cations, the overall surface charge of the adsorbent, and the speciation of phosphate in solution (Gan et al. 2009; Chouyyok et al. 2010). With pH values increasing from 2 to 12, the phosphate species was changed from H₂PO₄⁻ to HPO₄²⁻ (Karageorgiou et al. 2007; Chouyyok et al. 2010; Yang et al. 2013). The decreased P sorption capacity of B25 and B400 with increasing pH values could be explained by the ligand exchange mechanism (Collins et al. 1999). As the pH values increased from 3 to 11, HPO₄²⁻ becomes the predominant species, which was favorable for ligand exchange because the free energy for adsorption was lower than that of other species, and the P sorption capacity of the adsorbents decreased correspondingly (Lin et al. 2017). Moreover, high pH values could cause the bentonite surface to carry more OH⁻, which may lead to stronger competition between OH⁻ and HPO₄²⁻ on the bentonite surface in the solution (Su et al. 2013). But for B800, the high concentration of OH⁻ was the requirement for chemical precipitation of P because of the higher Ca²⁺ concentration. The results also showed that equilibrium pH values were much higher than initial pH values after the P adsorption process onto B25, B400, and B800 (Fig. 6), which proved that a ligand ion exchange process and metal hydroxylation occurred during the P adsorption process (Karageorgiou et al. 2007). The higher equilibrium pH value of the solution containing B800 than that solution containing B25 or B400 indicated that thermal treatment is an effective modification method for bentonite for phosphorus adsorption purposes.

Ca-bound P accounted for 75.5% of the total P, which indicated that the low concentrations of P removed by B800 were due mainly to precipitation. Previous studies have shown that P removed by soil colloids could be through precipitation (Liu et al. 2002), and it is considered to be an effective way to immobilize P into the Ca-P form for the control of phosphorus pollution in wastewater (Gan et al. 2009; Yin et al. 2011). With the strong Ca²⁺ release capacity, B800 supplied a large amount of dissolved Ca²⁺ to the solution, and the abundance of Ca²⁺ bound with P to form various Ca-P precipitates. The result showed that Ca₁₀-P had higher percentages than those of Ca₂-P and Ca₈-P in B800, which indicated that the binding force in Ca₁₀-P is stronger than that in Ca₂-P and Ca₈-P with high Ca²⁺ concentration in the solution. In addition, poorly crystallized or amorphous Ca₂-P and Ca₈-P can form as precursor phases in solutions containing Ca

and P, and they were recrystallized into thermodynamically stable $\text{Ca}_{10}\text{-P}$ over time (Valsami-Jones 2001; Kõiv et al. 2010).

Conclusions

With increasing calcination temperature, the crystal structure and physicochemical composition changed greatly and the BET surface area, pore volume values, and CEC increased, but decreased at the higher temperature. The maximum P sorption capacity of B800 was 6.94 mg P/g, higher than 0.24 mg P/g for B25 and 0.48 mg P/g for B400. With B800, more than 94% of P was rapidly (within 10 min) removed from low-phosphate concentrations. The Ca^{2+} release result showed that Ca^{2+} release capacity of B800 was 1.31 mg/g at the time of equilibrium, significantly higher than both B25 and B400 ($p < 0.05$), which indicated that high temperature can increase the release of calcium from bentonite clays. The initial pH value (3–11) has an important effect on phosphate removal efficiency for B25 and B400, but only a slight effect on P removal efficiency for B800. Phosphate fractionation analysis showed that the main fraction of the adsorbed P was Ca-bound P, which indicated that P removed by thermally treated bentonite at low-phosphorus concentration was a combination of $\text{Ca}_2\text{-P}$, $\text{Ca}_8\text{-P}$, and $\text{Ca}_{10}\text{-P}$. The findings indicated that thermal activation can effectively improve the capacity of bentonite to remove phosphate and B800 has the potential to be an efficient adsorbent for removing low-concentration phosphorus from wastewater.

Funding information This work was supported by the Key Research Project of Frontier Science of Chinese Academy of Sciences (QYZDJ-SSW-DQC041), the National Key Research and Development Program of China (2017YFD0800104 and 2016YFE0101100), the National Natural Science Foundation of China (41771302 and 41701566), the Youth Innovation Team Project of ISA, CAS (2017QNCXTD_LF), and the Key Research and Development Program of Hunan Province (2016JC2032).

References

- Al-Asheh S, Banat F, Abu-Aitah L (2003) Adsorption of phenol using different types of activated bentonites. *Sep Purif Technol* 33:1–10
- Aytas S, Yurtlu M, Donat R (2009) Adsorption characteristic of U(VI) ion onto thermally activated bentonite. *J Hazard Mater* 172:667–674
- Barca C, Gérente C, Meyer D, Chazarenc F, Andrès Y (2012) Phosphate removal from synthetic and real wastewater using steel slags produced in Europe. *Water Res* 46(7):2376–2384
- Barca C, Troesch S, Meyer D, Drissen P, Andres Y, Chazarenc F (2013) Steel slag filters to upgrade phosphorus removal in constructed wetlands: two years of field experiments. *Environ Sci Technol* 47(1):549–556
- Blanco I, Molle P, de Miera LES, Ansola G (2016) Basic oxygen furnace steel slag aggregates for phosphorus treatment. Evaluation of its potential use as a substrate in constructed wetlands. *Water Res* 89:355–365
- Brigatti MF, Galan E, Theng BKG (2013) Structure and mineralogy of clay minerals. In: Bergaya F, Lagaly G (eds) *Handbook of clay science*, Part A, 2nd edn. Elsevier, Amsterdam, pp 21–82
- Chen H, Zhao J, Zhong A, Jin Y (2011a) Removal capacity and adsorption mechanism of heat-treated palygorskite clay for methylene blue. *Chem Eng J* 174(1):143–150
- Chen T, Liu H, Li J, Chen D, Chang D, Kong D, Frost RL (2011b) Effect of thermal treatment on adsorption–desorption of ammonia and sulfur dioxide on palygorskite: change of surface acid-alkali properties. *Chem Eng J* 166:1017–1021
- Chen X, Zhou W, Pickett STA, Li W, Han L (2016a) Spatial-temporal variations of water quality and its relationship to land use and land cover in Beijing, China. *Int J Environ Res Public Health* 13:449
- Chen X, Zhou W, Pickett STA, Li W, Han L (2016b) Diatoms are better indicators of urban stream conditions: a case study in Beijing, China. *Ecol Indic* 60:265–274
- Chorom M, Rengasamy P (1996) Effect of heating on swelling and dispersion of different cationic forms of a smectite. *Clay Clay Miner* 44:783–790
- Chouyyok W, Wiacek RJ, Pattamakomsan K, Sangvanich T, Grudzien RM, Fryxell GE (2010) Phosphate removal by anion binding on functionalized nanoporous sorbents. *Environ Sci Technol* 44:3073–3078
- Collins CR, Ragnarsdottir KV, Sherman DM (1999) Effect of inorganic and organic ligands on the mechanism of cadmium sorption to goethite. *Geochim Cosmochim Acta* 63:2989–3002
- Elser JJ, Bracken ME, Cleland EE, Gruner DS, Harpole WS, Hillebrand H, Ngai JT, Seabloom EW, Shurin JB, Smith JE (2007) Global analysis of nitrogen and phosphorus limitation of primary producers in freshwater, marine and terrestrial ecosystems. *Ecol Lett* 10(12):1135–1142
- Emmerich K (2000) Spontaneous rehydroxylation of a dehydroxylated cis-vacant montmorillonite. *Clay Clay Miner* 48:405–408
- Gan F, Zhou J, Wang H, Du C, Chen X (2009) Removal of phosphate from aqueous solution by thermally treated natural palygorskite. *Water Res* 43(11):2907–2915
- Gupta SS, Bhattacharyya KG (2014) Adsorption of metal ions by clays and inorganic solids. *RSC Adv* 4(54):28537–28586
- Gupta VK, Carrott PJM, Ribeiro Carrott MML, Suhas (2009) Low-cost adsorbents: growing approach to wastewater treatment—a review. *Crit Rev Environ Sci Technol* 39(10):783–842
- Kaasik A, Vohla C, Mõtlp R, Mander Ü, Kirsimäe K (2008) Hydrated calcareous oil shale ash as potential filter media for phosphorus removal in constructed wetlands. *Water Res* 42:1315–1323
- Karageorgiou K, Paschalis M, Anastassakis GN (2007) Removal of phosphate species from solution by adsorption onto calcite used as natural adsorbent. *J Hazard Mater* 139:447–452
- Kõiv M, Liira M, Mander Ü, Mõtlp R, Vohla C, Kirsimäe K (2010) Phosphorus removal using Ca-rich hydrated oil shale ash as filter material—the effect of different phosphorus loadings and wastewater compositions. *Water Res* 44:5232–5239
- Lin J, Zhan Y, Wang H, Chu M, Wang C, He Y, Wang X (2017) Effect of calcium ion on phosphate adsorption onto hydrous zirconium oxide. *Chem Eng J* 309:118–129
- Liu F, Zhang S, Luo P, Zhuang X, Chen X, Wu J (2017) Purification and reuse of non-point source wastewater via *Myriophyllum*-based integrative biotechnology: a review. *Bioresour Technol* 248:3–11. <https://doi.org/10.1016/j.biortech.2017.07.181>
- Liu RX, Guo JL, Tang HX (2002) Adsorption of fluoride, phosphate and arsenate ions on a new type of ion exchange fiber. *J Colloid Interface Sci* 248:268–274
- Loganathan P, Vigneswaran S, Kandasamy J, Bolan NS (2014) Removal and recovery of phosphate from water using sorption. *Crit Rev Environ Sci Technol* 44(8):847–907
- Luo P, Liu F, Liu X, Wu X, Yao R, Chen L, Li X, Xiao R, Wu J (2017) Phosphorus removal from lagoon-pretreated swine wastewater by

- pilot-scale surface flow constructed wetlands planted with *Myriophyllum aquaticum*. *Sci Total Environ* 576:490–497
- Ortega LH (2009) Sintered bentonite ceramics for the immobilization of cesium- and strontium-bearing radioactive waste. Texas A&M University, Texas, pp 33–42
- Önal M, Sarıkaya Y (2007) Thermal behavior of a bentonite. *J Therm Anal Calorim* 90(1):167–172
- Rentz JA, Turner IP, Ullman JL (2009) Removal of phosphorus from solution using biogenic iron oxides. *Water Res* 43:2029–2035
- Sarıkaya Y, Önal M, Baran B, Alemdaroğlu T (2000) The effect of thermal treatment on some of the physicochemical properties of a bentonite. *Clay Clay Miner* 48(5):557–562
- Sengupta S, Pandit A (2011) Selective removal of phosphorus from wastewater combined with its recovery as a solid-phase fertilizer. *Water Res* 45:3318–3330
- Soil Science Society of China (2002) Soil agrochemistry analysis method. China Agricultural Press, Beijing
- Stagnaro SYM, Volzone C, Rueda ML (2012) Influence of thermal treatment on bentonite used as adsorbent for Cd, Pb, Zn retention from mono-solute and poly-solute aqueous solutions. *Mater Res* 15:1–5
- Su Y, Cui H, Li Q, Gao SA, Shang JK (2013) Strong adsorption of phosphate by amorphous zirconium oxide nanoparticles. *Water Res* 47:5018–5026
- Tămășan M, Vulpoi A, Vanea E, Simon V (2010) Textural properties of the medical Algo clay as influenced by calcination. *Appl Clay Sci* 50:418–422
- Tan KH (1996) Soil sampling, preparation and analysis. Marcel Dekker Inc., New York
- Toor M, Jin B (2012) Adsorption characteristics, isotherm, kinetics, and diffusion of modified natural bentonite for removing diazo dye. *Chem Eng J* 187:79–88
- Tran HN, You SJ, Hosseini-Bandegharai A, Chao HP (2017) Mistakes and inconsistencies regarding adsorption of contaminants from aqueous solutions: a critical review. *Water Res* 120:88–116
- Valsami-Jones E (2001) Mineralogical controls on phosphorus recovery from wastewaters. *Mineral Mag* 65(5):611–620
- Vimonses V, Lei S, Jin B, Chow C, Saint C (2009) Adsorption of Congo red by three Australian kaolins. *Appl Clay Sci* 43:465–472
- Vohla C, Köiv M, Bavor HJ, Chazarenc F, Mander Ü (2011) Filter materials for phosphorus removal from wastewater in treatment wetlands—a review. *Ecol Eng* 37(1):70–89
- Walter WJ (1984) Evolution of a technology. *J Environ Eng* 110(5):899–917
- Weber WJ, Smith EH (1987) Simulation and design models for adsorption processes. *Environ Sci Technol* 21(11):1040–1050
- Wei XC, Viadero JRC, Bhojappa S (2008) Phosphorus removal by acid mine drainage sludge from secondary effluents of municipal wastewater treatment plants. *Water Res* 42:3275–3284
- Yang S, Zhao Y, Ding D, Wang Y, Feng C, Lei Z, Yang Y, Zhang Z (2013) An electrochemically modified novel tablet porous material developed as adsorbent for phosphate removal from aqueous solution. *Chem Eng J* 220:367–374
- Ye HP, Chen FZ, Sheng YQ, Sheng GY, Fu JM (2006) Adsorption of phosphate from aqueous solution onto modified palygorskites. *Sep Purif Technol* 50:283–290
- Yeoman S, Stephenson T, Lester JN, Perry R (1988) The removal of phosphorus during wastewater treatment: a review. *Environ Pollut* 49:183–233
- Yin H, Han M, Tang W (2016) Phosphorus sorption and supply from eutrophic lake sediment amended with thermally-treated calcium-rich attapulgite and a safety evaluation. *Chem Eng J* 285:671–678
- Yin H, Yan X, Gu X (2017) Evaluation of thermally-modified calcium-rich attapulgite as a low-cost substrate for rapid phosphorus removal in constructed wetlands. *Water Res* 115:329–338
- Yin H, Yun Y, Zhang Y, Fan C (2011) Phosphate removal from wastewaters by a naturally occurring, calcium-rich sepiolite. *J Hazard Mater* 198:362–369
- Zhu R, Chen Q, Zhou Q, Xi Y, Zhu J, He H (2016) Adsorbents based on montmorillonite for contaminant removal from water: a review. *Appl Clay Sci* 123:239–258
- Zhu R, Zhu L, Zhu J, Ge F, Wang T (2009) Sorption of naphthalene and phosphate to the CTMAB-A113 intercalated bentonites. *J Hazard Mater* 168:1590–1594
- Zuo Q, Gao X, Yang J, Zhang P, Chen G, Li Y, Shi K, Wu W (2017) Investigation on the thermal activation of montmorillonite and its application for the removal of U(VI) in aqueous solution. *J Taiwan Inst Chem Eng* 80:754–760